

Article

Study of a Novel Hybrid Refrigeration System, with Natural Refrigerants and Ultra-Low Carbon Emissions, for Air Conditioning

Yijian He ^{1,*}, Yufu Zheng ², Jianguang Zhao ², Qifei Chen ¹ and Lunyuan Zhang ¹

¹ Institute of Refrigeration and Cryogenics, Zhejiang University, Hangzhou 310027, China; 21927101@zju.edu.cn (Q.C.); 22360530@zju.edu.cn (L.Z.)

² Zhejiang Shike Auto Parts Co., Ltd., Lishui 323799, China; anny.ni@shikeparts.com (Y.Z.); leo.fang@shikeparts.com (J.Z.)

* Correspondence: yijian_he@zju.edu.cn

Abstract: Due to its environmental benefits, CO₂ shows great potential in refrigeration systems. However, a basic CO₂ transcritical (BCT) refrigeration system used for airconditioning in buildings might generate massive indirect carbon emissions for its low COP. In this study, a novel CO₂ transcritical/two-stage absorption (CTTA) hybrid refrigeration system is broadly investigated, and both energy efficiency and life cycle climate performance (LCCP) are specifically engaged. The theoretical model shows that optimal parameters for the generator inlet temperature (T_{G2}), intermediate temperature (T_m), and discharge pressure (P_c), exist to achieve maximum COP_{tot}. Using the LCCP method, the carbon emissions of the CTTA system are compared to six typical refrigeration systems by using refrigerants, including R134a, R1234yf and R1234ze(E) etc. The LCCP value of the CTTA system is 3768 kg CO_{2e}/kW, which is 53.6% less than the BCT system and equivalent to the R134a system. Moreover, its LCCP value could be 3.4% less than the R1234ze(E) system if the COP of the CO₂ subsystem is further improved. In summary, the CTTA system achieves ultra-low carbon emissions, which provides a potential alternative to air conditioning systems in buildings that can be considered alongside R1234yf and R1234ze(E) systems.

Keywords: airconditioning; energy efficiency; natural refrigerant; low carbon emission



Citation: He, Y.; Zheng, Y.; Zhao, J.; Chen, Q.; Zhang, L. Study of a Novel Hybrid Refrigeration System, with Natural Refrigerants and Ultra-Low Carbon Emissions, for Air Conditioning. *Energies* **2024**, *17*, 880. <https://doi.org/10.3390/en17040880>

Academic Editor: Francesco Minichiello

Received: 2 January 2024

Revised: 31 January 2024

Accepted: 6 February 2024

Published: 14 February 2024



Copyright: © 2024 by the authors. Licensee MDPI, Basel, Switzerland. This article is an open access article distributed under the terms and conditions of the Creative Commons Attribution (CC BY) license (<https://creativecommons.org/licenses/by/4.0/>).

1. Introduction

In the past few years, energy consumption in the building sector has exploded as a result of urbanization and economic development. According to the International Energy Agency, global final energy consumption will increase by 60% in the building sector, bringing corresponding environmental challenges, such as carbon emissions [1]. Air conditioning is an essential addition to most commercial buildings, although it is more widely used in residences. However, such systems consume large amounts of power and generate massive carbon emissions. Air conditioning systems and heat pumps account for about 7.8% of global carbon emissions [2]. Environmental concerns and the development of low carbon emission buildings have led to restrictions on widely used high GWP refrigerants such as R134a, which pose serious challenges to the transformation and upgrading of the air conditioning industry and buildings. Environmentally friendly refrigerants with high energy efficiency have attracted attentions as a way to reduce carbon emissions [3]. As alternative refrigerants, R32, R1234yf, R1234ze(E), R513a, R450a, R744a (N₂O) and R744 (CO₂), have been gradually investigated by those with an interest in developing refrigeration systems for air conditioning. The main properties of these refrigerants are listed in Table 1.

Table 1. Main properties of typical refrigerants [4].

Characteristic	R744	R744a	R134a	R32	R1234yf	R1234ze(E)	R513a	R450a
ODP	0	0	0	0	0	0	0	0
GWP	1	240	1300	675	<1	4	572	547
Critical temperature/°C	31.0	36.4	101.1	78.4	94.7	109.4	94.9	104.5
Critical pressure/MPa	7.4	7.3	4.1	5.8	3.4	3.6	3.7	3.8
Boiling point/°C	−78.5	−88.5	−26.1	−51.6	−29.5	−19.0	−29.8	−23.4
Standard safety classification	A1	/	A1	A2	A2L	A2L	A1	A1

Compared to a R134a system, the study of R32 refrigeration systems showed a 5–7% increase in COP [5]. The GWP of R32 is relatively high, and so more environmental-friendly refrigerant alternatives are expected to emerge and take its place. R1234yf and R1234ze(E) have been suggested as promising refrigerants for their extremely low GWP and excellent thermal properties, despite their relatively high cost [6]. Joaquin et al. conducted a theoretical and experimental study of a R1234yf refrigeration system with internal heat exchanger (IHX) [7]. Although the IHX improved the COP by 2–6%, the COP of the R1234yf system was still 6–13% lower than that of the R134a system in air conditioning conditions. Considering the GWP of the refrigerant and its system COP, both R513a (a mixture of R134a and R1234yf) and R450a (a mixture of R134a and R1234ze(E)) have been considered as alternatives to R134a, as they both have similar thermal properties and relatively low GWP that have been studied. And carbon emissions have, over the life cycle of the system, been increasingly used to assess the environmental impacts [8]. A substitution study of R450a and R513a showed that R513a had a slightly higher COP than the R450a system for air conditioning [2,9]. Compared to the R134a system, their direct carbon emissions were reduced by 50–52% for lower GWP and less refrigerant leakage. The carbon emissions of refrigeration systems during their life cycle need to be considered by referring to several sources, such as refrigerant leakage, electricity consumption and manufacturing processes, etc.

The International Institute of Refrigeration (IIR) developed the life cycle climate performance (LCCP) method to evaluate all the direct and indirect carbon emissions of a refrigeration system during its life cycle [10], and it is widely used in comparisons between different refrigerants or refrigeration systems [11,12]. In the literature [2,9], when the carbon emissions generated by energy consumption are taken into account, the carbon emissions of the R513a system are equivalent to the R134a system, while the R450a system is 4.8% higher. In the transformation and upgrading of air conditioning systems, it is essential to not only focus on the use of 0 ODP and low GWP refrigerants, but to also obtain advantages, in terms of life cycle carbon emissions. The above studies imply that refrigerant alternatives are still confronted by challenges, and that the development of new alternative refrigeration will be an essential priority for future research.

Natural refrigerants have received widespread attention in the research of air conditioning systems. Of them, CO₂ (R744) is recognized as a non-flammable and non-toxic attractive option, with superior properties such as extremely low GWP, low production cost, and high thermal conductivity [13]. Because of a relatively low COP, a basic CO₂ transcritical (BCT) refrigeration cycle has still not been adapted for air conditioning in buildings. Researchers have paid attention to the parameter optimization and cycle innovation of CO₂ transcritical refrigeration systems. Zheng et al. studied the CO₂ mass migration and distribution of an air conditioning system and found that an appropriate charge could improve the COP by 10.1% [14]. In a subcooler-based CO₂ transcritical system, it was found that optimizing compressor discharge pressure increased the COP by 8.8% [15]. Moreover, advanced cycles have been found to significantly affect the improvement of COP. A CO₂ ejector refrigeration cycle for air conditioning proposed by Lawrence et al. improved the COP by 20% [16]. Tashtoush et al. proposed an ejector-cascade refrigeration

cycle for air conditioning; when compared to the BCT cycle, this new cycle improved the COP by 30% [17,18]. From an environmental perspective, the improvement in COP shows the potential of CO₂ refrigeration in low carbon buildings. An energy and environmental analysis of a CO₂ heat pump system shows that its COP competes with a R134a system, reducing total carbon emissions by 52.05%, while maintaining a lower COP in cooling mode [19]. A further study of the air conditioning performance of CO₂ refrigeration systems is however necessary.

Input power converted to high temperature heat at the outlet of the gas cooler is one of the limitations leading to low COP, and the high temperature heat might need to be recovered. Efficient absorption refrigeration systems have the advantage of low-grade heat recovery and use natural refrigerants as well. Hybrid refrigeration systems that combine absorption and vapor compression refrigeration systems have the potential to improve overall energy efficiency and reduce carbon emissions. Chan et al. developed a hybrid system for cooling by driving an absorption refrigeration system with condensing heat recovery, resulting in a 53% reduction in carbon emissions [20]. Similarly, Jain et al. developed a vapor compression-absorption hybrid refrigeration system, with power consumption 170.4% lower than a vapor compression system [21]. Andrej et al. used the heat from the CO₂ compressor outlet to drive an adsorption chiller [22]. The hybrid system showed 22% annual energy savings. These studies suggest that coupling a CO₂ transcritical refrigeration system with an absorption refrigeration system may lead to a reduction in overall carbon emissions, and also that the application of CO₂ to air conditioning in low carbon buildings shows promise.

In our previous work, thermodynamic analyses of a two-stage absorption/transcritical hybrid refrigeration system was conducted [23]. The high-pressure generator of the absorption subsystem is driven by the waste heat from the gas cooler outlet. The hybrid system converts waste heat as low as 45–55 °C into useful cooling of 7 °C, and uses a rational coupling method to recover the gas cooler waste heat with the absorption system. Further research should investigate the potential of the low-pressure generator to recover the waste heat and carbon emission reductions.

In this study, a novel CO₂ transcritical/two-stage absorption (CTTA) hybrid refrigeration system for air conditioning is conducted on the basis of both COP and LCCP value. A simulation model of the CTTA system is established and calculated by EES [24] and the effects of key parameters on the COP are analyzed. Its carbon emissions are evaluated by using the LCCP method and are then compared with six typical refrigeration systems by using R744 (CO₂), R134a, R32, R450a, R513a, R1234yf, and R1234ze(E) as refrigerants, respectively. Finally, the potential LCCP values of the CTTA system are estimated to demonstrate the prospect it can be applied to low carbon emission buildings in the future.

2. Descriptions of the CTTA System and Theoretical Model

2.1. Descriptions of the CTTA System

Based on the previous investigations [23], further modification is adopted and a new CO₂ transcritical/two-stage absorption (CTTA) hybrid refrigeration system for air conditioning is proposed, which also mainly consists of two subsystems, namely the two-stage absorption refrigeration subsystem and the CO₂ transcritical refrigeration sub-system, as shown in the schematic of Figure 1. Its main components contain generator1 (G1), condenser (C), throttling valve 1 (TV1), condensing subcooler (CS), absorber1 (AB1), solution pump 1 (SP1), solution heat exchanger 1 (SHX1), TV2, G2, TV3, evaporator (E), AB2, SP2, SHX2, TV4, compressor (COMP), gas cooler (GC), IHX and TV5. Furthermore, its P-T diagram is shown as Figure 2. From the P-T diagram, it is easy to find the main difference between the new system and the previous one [23], where the two-stage absorption refrigeration system is depicted with a dotted line. There is important difference in the process of the CO₂ transcritical refrigeration subsystem for the new system, where the discharged heat at high pressure of the CO₂ transcritical refrigeration subsystem not only involves G1 but also G2, and the discharged heat at an extended temperature range is effectively utilized

to generate refrigeration without external input heat. As a result, the energy efficiency of the input power to refrigeration is obviously lifted. Accordingly, involved thermodynamic states obviously change, as shown in Figure 2. For example, a decrease in the intermediate pressure of the absorption refrigeration subsystem results in an increase in the concentration of the concentrated solution in G2 and the dilute solution in G1. Consequently, the decrease in the generation temperature of G2 (TG2) in similar operating conditions demonstrates the good potential for exhaust heat from the CO₂ subsystem to be utilized. Similarly, there is an increase in the concentration difference at G2, while the concentration difference at G1 decreases.

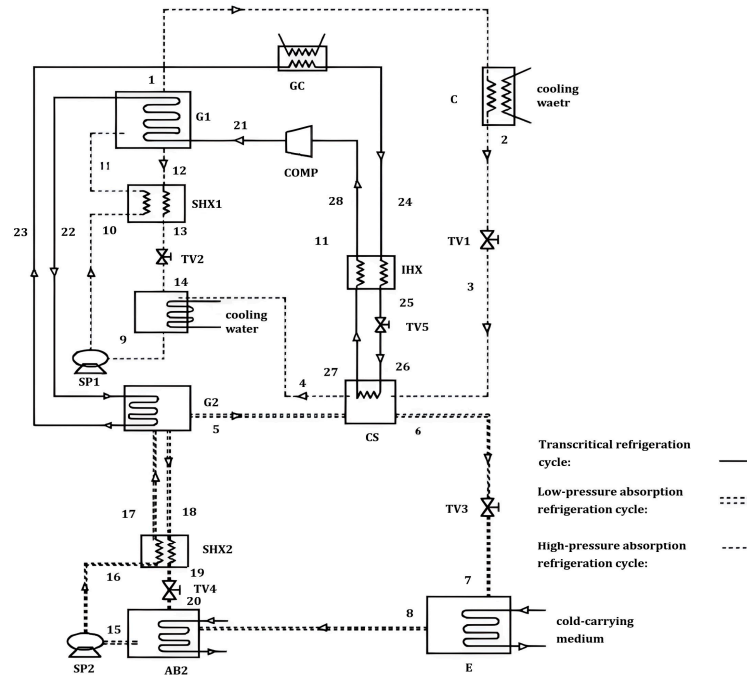


Figure 1. Schematic of the CTTA system.

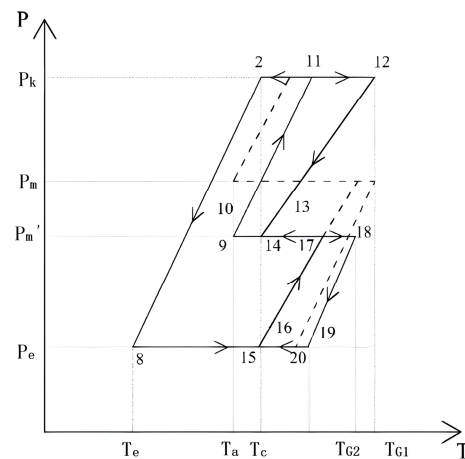


Figure 2. Comparison of a new two-stage absorption refrigeration subsystem and normal two-stage absorption refrigeration system, in a P-T diagram.

CO₂ transcritical refrigeration subsystem: In COMP, CO₂ is compressed into high-temperature and high-pressure steam (state point 21). It then enters G1 and a large amount of heat is transferred to the LiBr solution (state point 22). The outlet temperature of CO₂ at G1 is still high enough to enter G2 and transfer the heat to the LiBr solution (state point 23). After the temperature of CO₂ is further reduced at G2, it enters the GC to

get cooled (state point 24), before entering IHX for heat exchange with the vapor from E (state point 25). CO₂ is throttled by TV5 (state point 26) and then enters CS and IHX for heat absorption (state point 28). Finally, CO₂ is compressed by COMP to complete the transcritical refrigeration cycle.

Water working cycle: Heat exchange between LiBr solution and CO₂ in G1 generates high-temperature and high-pressure water vapor (state point 1). The vapor is cooled by water in C and is throttled by TV1 to CS. Similarly, the LiBr solution in G2 generates high-temperature and high-pressure vapor after absorbing exhaust heat from the outlet of G1 (state point 5). The water vapor goes directly into CS, mixes with water vapor from G1, and exchanges heat with CO₂. The liquid refrigerant in the condensing subcooler (state point 6) is throttled by TV3 and then enters E (state point 7) for heat absorption and producing refrigeration capacity, before entering AB2 (state point 8) and being absorbed by the concentrated solution. The refrigerant vapor (state point 4) then enters AB1 and is absorbed by the concentrated solution.

Solution working cycle: After the LiBr solution's concentration increases in G1 (state point 12), it enters SHX1 and is cooled (state point 13) through TV 2 (state point 14), then enters AB1m, absorbing water vapor into a dilute solution (state point 9); after this, it then enters into the SHX1 (state point 10) and exchanges heat with concentrated solution from G1, before finally being returned to G1 (state point 11).

2.2. Construction of the Simulation Model

Herold established a steady-state model for a single effect absorption refrigeration system, which uses LiBr-H₂O as the working fluids [25]. The model worked on the assumptions that there was only condensing and evaporation pressure in the entire system and the working fluids in the generator and absorber were in a state of equilibrium. He et al. established a thermodynamic model of a hybrid system of liquid desiccant and CO₂ transcritical cycles [26], and used a similar approach to establish a steady-state simulation model of the CTTA system. The process of simulation is as follows: first, establish a mathematical model for each component of the system and verify the model. Then, combine these models under the designed working conditions. The design conditions of the CTTA system are listed in Table 2. Finally, the input parameters are changed sequentially to analyze the CTTA system performance.

Table 2. Designing conditions of the CTTA system.

Parameter	Value	Unit
Inlet temperature of CO ₂ in G1	80	°C
Inlet temperature of cooling water for condenser and absorber	32	°C
Inlet temperature of air	32	°C
Outlet temperature of chilled water	9	°C
Temperature at subcooler	18	°C
Condensing temperature	35	°C
Absorption temperature	35	°C
Evaporating temperature	7	°C
Discharged pressure	9.7	MPa

In the simulation process, the system is assumed to be steady-state and several assumptions are made to simplify the model:

1. The water vapor mass flow rates from G1 and G2 are equivalent to the mass flow rates from AB1 and AB2, respectively.
2. The power consumption of the solution pumps is not factored into the analysis.
3. All throttling processes are assumed to be isenthalpic.
4. The outlet solution from the generator and absorber is saturated.
5. The heat loss along the pipeline is disregarded.

6. The pressure drop in the pipes and heat exchangers of the absorption subsystem is negligible.
7. The isentropic efficiency of the compressor is taken as 0.8.
8. The outlet solution temperature of the generator is the generation temperature and the outlet dilute solution temperature of the absorber is the absorption temperature.

Based on the above assumptions, the control equations for each component are as follows:

$$G1 : \dot{m}_1 \cdot h_1 + \dot{m}_{12} \cdot h_{12} = \dot{m}_{11} \cdot h_{11} + Q_{G1} \quad (1)$$

$$Q_{G1} = \dot{m}_{21} \cdot h_{21} - \dot{m}_{22} \cdot h_{22} \quad (2)$$

$$\dot{m}_{11} = \dot{m}_1 + \dot{m}_{12} \quad (3)$$

$$\dot{m}_{11} \cdot x_{11} = \dot{m}_1 \cdot x_1 + \dot{m}_{12} \cdot x_{12} \quad (4)$$

$$C : \dot{m}_1 \cdot h_1 = \dot{m}_2 \cdot h_2 + Q_c \quad (5)$$

$$\dot{m}_1 = \dot{m}_2 \quad (6)$$

$$TV1 : \dot{m}_2 \cdot h_2 = \dot{m}_3 \cdot h_3 \quad (7)$$

$$\dot{m}_2 = \dot{m}_3 \quad (8)$$

$$AB1 : \dot{m}_4 \cdot h_4 + \dot{m}_{14} \cdot h_{14} = \dot{m}_9 \cdot h_9 + Q_{AB1} \quad (9)$$

$$\dot{m}_4 + \dot{m}_{14} = \dot{m}_9 \quad (10)$$

$$\dot{m}_4 \cdot x_4 + \dot{m}_{14} \cdot x_{14} = \dot{m}_9 \cdot x_9 \quad (11)$$

$$SP1 : \dot{m}_{10} \cdot h_{10} = \dot{m}_9 \cdot h_9 + W_{SP1} \quad (12)$$

$$\dot{m}_9 = \dot{m}_{10} \quad (13)$$

$$SHX1 : \dot{m}_{12} \cdot h_{12} - \dot{m}_{13} \cdot h_{13} = \dot{m}_{11} \cdot h_{11} - \dot{m}_{10} \cdot h_{10} \quad (14)$$

$$\dot{m}_{10} = \dot{m}_{11} \quad (15)$$

$$\dot{m}_{12} = \dot{m}_{13} \quad (16)$$

$$TV2 : \dot{m}_{13} \cdot h_{13} = \dot{m}_{14} \cdot h_{14} \quad (17)$$

$$\dot{m}_{13} \cdot h_{13} = \dot{m}_{14} \cdot h_{14} \quad (18)$$

$$G2 : \dot{m}_{18} \cdot h_{18} + \dot{m}_5 \cdot h_5 = \dot{m}_{17} \cdot h_{17} + Q_{G2} \quad (19)$$

$$\dot{m}_{18} + \dot{m}_5 = \dot{m}_{17} \quad (20)$$

$$\dot{m}_{18} \cdot x_{18} + \dot{m}_5 \cdot x_5 = \dot{m}_{17} \cdot x_{17} \quad (21)$$

$$TV3 : \dot{m}_6 \cdot h_6 = \dot{m}_7 \cdot h_7 \quad (22)$$

$$\dot{m}_6 = \dot{m}_7 \quad (23)$$

$$E : \dot{m}_8 \cdot h_8 = \dot{m}_7 \cdot h_7 + Q_E \quad (24)$$

$$\dot{m}_8 = \dot{m}_7 \quad (25)$$

$$\text{AB2} : \dot{m}_8 \cdot h_8 + \dot{m}_{20} \cdot h_{20} = \dot{m}_{15} \cdot h_{15} + Q_{\text{AB2}} \quad (26)$$

$$\dot{m}_8 \cdot x_8 + \dot{m}_{20} \cdot x_{20} = \dot{m}_{15} \cdot x_{15} \quad (27)$$

$$\dot{m}_8 + \dot{m}_{20} = \dot{m}_{15} \quad (28)$$

$$\text{SHX2} : \dot{m}_{18} \cdot h_{18} - \dot{m}_{19} \cdot h_{19} = \dot{m}_{17} \cdot h_{17} - \dot{m}_{16} \cdot h_{16} \quad (29)$$

$$\dot{m}_{16} = \dot{m}_{17} \quad (30)$$

$$\dot{m}_{18} = \dot{m}_{19} \quad (31)$$

$$\text{TV4} : \dot{m}_{19} \cdot h_{19} = \dot{m}_{20} \cdot h_{20} \quad (32)$$

$$\dot{m}_{19} = \dot{m}_{20} \quad (33)$$

$$\text{COMP} : \dot{m}_{21} \cdot h_{21} = \dot{m}_{27} \cdot h_{27} + W_c \quad (34)$$

$$\dot{m}_{21} = \dot{m}_{27} \quad (35)$$

$$\text{GC} : \dot{m}_{22} \cdot h_{22} - \dot{m}_{23} \cdot h_{23} = Q_{\text{GC}} \quad (36)$$

$$\dot{m}_{22} = \dot{m}_{23} \quad (37)$$

$$\text{IHX} : \dot{m}_{23} \cdot h_{23} - \dot{m}_{24} \cdot h_{24} = \dot{m}_{27} \cdot h_{27} - \dot{m}_{26} \cdot h_{26} \quad (38)$$

$$\dot{m}_{23} = \dot{m}_{24} \quad (39)$$

$$\dot{m}_{26} = \dot{m}_{27} \quad (40)$$

$$\text{TV5} : \dot{m}_{24} \cdot h_{24} = \dot{m}_{25} \cdot h_{25} \quad (41)$$

$$\dot{m}_{24} = \dot{m}_{25} \quad (42)$$

$$\text{CS} : \dot{m}_3 \cdot h_3 + \dot{m}_5 \cdot h_5 = \dot{m}_4 \cdot h_4 + \dot{m}_6 \cdot h_6 + \dot{m}_{26} \cdot h_{26} - \dot{m}_{25} \cdot h_{25} \quad (43)$$

$$\dot{m}_{25} = \dot{m}_{26} \quad (44)$$

$$\dot{m}_3 + \dot{m}_5 = \dot{m}_4 + \dot{m}_6 \quad (45)$$

The thermal properties of the LiBr-H₂O pair are vital for calculating the performance of the absorption refrigeration subsystem. Mcneely carried out several studies of the thermal properties of the LiBr solution and produced empirical formulas for computing its thermal properties [27]. The formula applies to a concentration range of 0% to 70% and a temperature range of 4.4 °C to 121 °C. Therefore, the thermal properties of the LiBr solution reference Mcneely's study, and the equations used to calculate the thermal properties of H₂O are taken from IAPWS-95 [28]. The thermal property of CO₂ is calculated by using correlations proposed by Span and Wagner in 1996 [29]. The heat transfer of the refrigerant in the absorption refrigeration subsystem is calculated by drawing on correlations from the literature [30]. The heat transfer of CO₂ in smooth tubes is calculated by using the correlation given by Pital and the pressure drop is calculated by using the correlation given by Wang [31,32]. The heat transfer of CO₂ in the boiling zone is calculated by using the

correlation given by Wattlelet-Carle and the pressure drop is calculated according to the correlation given by Lockhart-Martinelli [33,34].

Various evaluation criteria have been proposed by researchers for hybrid refrigeration systems. In this context, two criteria are used. COP_{tol} represents the overall coefficient of performance of the CTTA system, which is the ratio of the total refrigeration capacity (Q_e , kW) to the mechanical work (W , kW) consumed by COMP.

$$COP_{tol} = Q_e / W \quad (46)$$

Another evaluation criterion, COP_{ch} , is proposed to evaluate the performance of a conventional hybrid refrigeration system, where the generators are not coupled to GC. Where COP_a represents the COP that a conventional two-stage absorption refrigeration system can achieve under the same operating conditions, without coupling a CO₂ system

$$COP_{ch} = (Q_e - (Q_{G1} + Q_{G2}) \cdot COP_a) / W \quad (47)$$

To compare the environmental advantages of the CTTA system, the direct and indirect carbon emissions of the system are calculated by using the LCCP method.

$$LCCP = Direct\ Emissions + Indirect\ Emissions \quad (48)$$

Direct emissions are the effects of refrigerants released into the atmosphere over the lifetime of the unit and afterwards. It is calculated in kg CO_{2e}/kW, as the ratio of Direct emissions to the total refrigeration capacity:

$$Direct\ Emissions = [Cr \cdot (L \cdot ALR + EOL) \cdot (GWP + Adp \cdot GWP)] / Q_e \quad (49)$$

Indirect carbon emissions account for all other sources of power generation, material manufacturing, and equipment disposal during the life cycle. It is calculated in kg CO_{2e}/kW, as the ratio of Indirect emissions to the total refrigeration capacity:

$$Indirect\ Emissions = L \cdot AEC \cdot EM + \sum (M \cdot MM) + \sum (mr \cdot RM) + Cr \cdot (1 + ALR) \cdot RFM + Cr \cdot (1 - EOL) \cdot RFD \quad (50)$$

3. Validation of the Performance Simulation Model

Based on the simulation models and the designing working conditions, the structure parameters of each component used in the CTTA system are listed in Table 3. The simulation models of the CTTA system are solved by using EES, RefProp and Matlab/Simulink programs, and are validated by using experimental data from the literature [35,36].

Table 3. The structural parameters of each component.

Component	Parameters
The CO ₂ subsystem	
COMP	the special piston compressor for CO ₂ , $V_{th} = 2.7 \text{ m}^3/\text{h}$, rated input power: 3 kW, rated speed: 1450 rpm
GC	Fin-tube heat exchanger, diameter: $7 \times 0.35 \text{ mm}$, fin thickness: 0.15 mm, fin pitch: 2 mm, tube spacing: 21 mm
IHX	Double tube heat exchanger, diameter: $6 \times 0.5 \text{ mm}$, $10 \times 1 \text{ mm}$
CS	Tube heat exchanger, diameter: $8 \times 1 \text{ mm}$
The absorption subsystem	
G1	Immersive serpentine coil heat exchanger, diameter: $8 \times 1 \text{ mm}$
G2	Immersive serpentine coil heat exchanger, diameter: $6 \times 0.5 \text{ mm}$
E	Shell and tube heat exchanger, diameter: $8 \times 1 \text{ mm}$
C	Shell and tube heat exchanger, diameter: $8 \times 1 \text{ mm}$
AB1	Shell and tube heat exchanger, diameter: $6 \times 0.5 \text{ mm}$
AB2	Shell and tube heat exchanger, diameter: $10 \times 1 \text{ mm}$
SHX1	Double tube heat exchanger, diameter: $8 \times 1 \text{ mm}$
SHX2	Double tube heat exchanger, diameter: $6 \times 0.5 \text{ mm}$

In a hybrid refrigeration system, theoretical model verification is conducted separately for subsystem models; for example, Mohammadi validated the proposed hybrid system of CO₂ transcritical system and an absorption system separately [37]. The calculated results are in agreement with the published data and the difference is within the permitted limits. The same validation approach is adopted by Farsi et al. for a hybrid system, which consists of a CO₂ transcritical system and multi-effect desalination system [38]. The calculated results are in agreement with the validation data, and the maximum diversity is 6.6% in similar working conditions. The preceding results show that the hybrid system models can be verified by individual verification of the subsystems.

In this context, the simulation results of the absorption refrigeration subsystem are compared to the published experimental data in the literature [21,39], respectively. The convergence accuracy of the model is set as 0.5%. Figure 3 compares the COP and the Q_e to [21,39]. The simulation results and the experimental data show good agreement. The simulation results of the COP (COP_{sim}) are 4~6% higher than that of the experiment (COP_{exp}). The simulation results of the $Q_{e,sim}$ are 1~4% higher than the $Q_{e,exp}$. The neglect of the heat leakage of each heat exchanger and other relevant factors in the simulation processes induces the deviation.

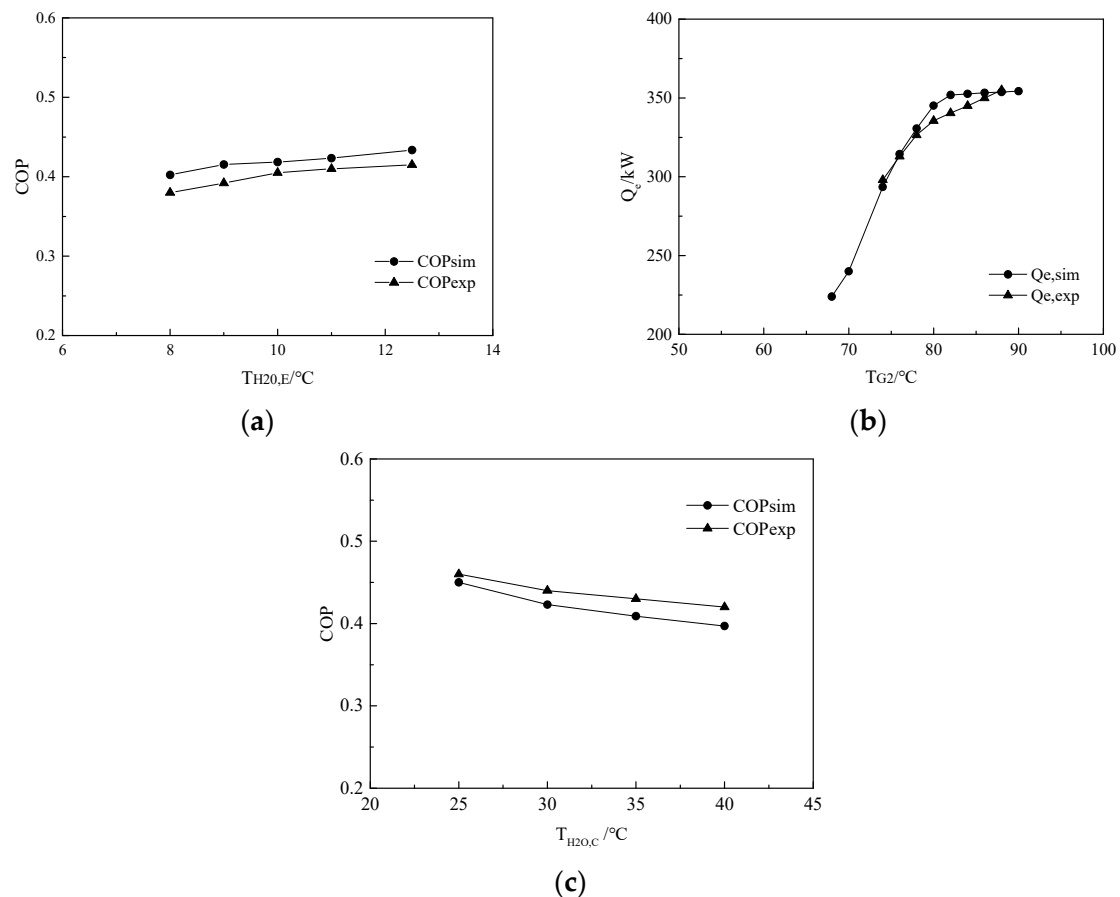


Figure 3. Comparisons of the simulation and experimental results: (a) COP- T_E (b) Q_e - T_{G2} (c) COP- T_C .

Comparisons of the experimental data and the calculation show the maximum deviation is calculated at 8.6%, and the average deviation is calculated at 4.5%, which implies the reliability of the chosen empirical correlations and the simulation models of the CO₂ subsystem. On the basis of the validation results of each subsystem, we also conclude the simulation models of the CTTA system show an ability to predict main performance and characteristics.

4. Results and Discussion

The performance of the transcritical refrigeration subsystem is first compared by using CO_2 and N_2O as refrigerants. T_{G1} and T_{G2} are $55\text{ }^\circ\text{C}$ and $52\text{ }^\circ\text{C}$, respectively, and other operating parameters are the same as those listed in Table 2.

As shown in Figure 4, both COP_{tot} and COP_{ch} of the N_2O subsystem decrease with the increase of discharge pressure (P_c), while the CO_2 subsystem first increases and then decreases because of its thermal property change near the critical point. As the exhaust pressure increases, both the power consumption and the cooling capacity of the transcritical subsystem increase. At the same time, the increase in the cooling capacity of the transcritical subsystem causes the water vapor to be gradually and completely condensed in the condensing subcooler, resulting in an increase in the cooling capacity of the CTTA system. Since the CTTA system consists of a coupled two-stage absorption refrigeration subsystem and a transcritical heat pump subsystem, it is driven by both external low-grade energy and mechanical work. When the P_c is higher than the optimal value for this operating condition, the cooling capacity generated by the input mechanical work is increasing, leading to a decrease in the COP of the CTTA system.

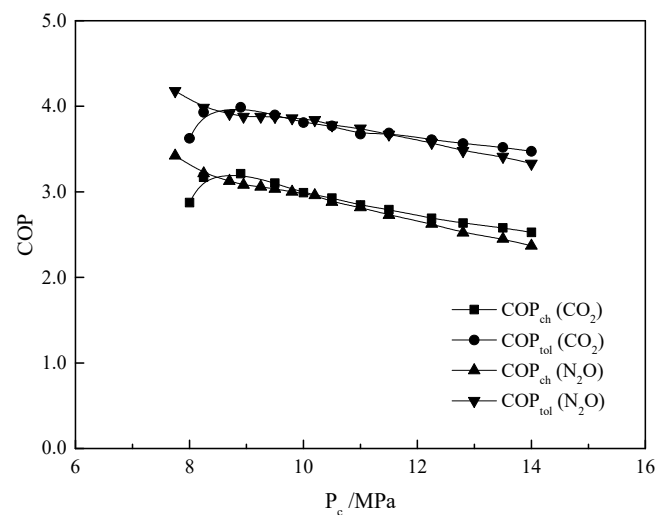


Figure 4. Effects of P_c on the performance, using different refrigerants.

COP using CO_2 is higher than that using N_2O when the discharge pressure is higher than 8.3 MPa and the GWP of N_2O is higher than CO_2 . So the novel hybrid system uses CO_2 as the refrigerant and the simulation is carried out in different working conditions, and the other designing parameters are the same as those listed in Table 2.

In order to analyze the COP improvement of the hybrid system, a BCT refrigeration system with IHX previously examined by Zhang et al. is used as a comparison [40]. The maximum COP obtained for this BCT system is 2.75 when the T_E is $10\text{ }^\circ\text{C}$, the gas cooler outlet temperature is $20\text{ }^\circ\text{C}$, and the P_c is 10 MPa ; in this study, it is named COP_t .

CS is a key component of the CTTA system that was introduced in our previous study [23]. The effect of T_m on COP_{tot} is first investigated, and the results are shown in Figure 5. The other parameters are the same as those of the design conditions. Figure 5 shows that there is a maximum COP_{tot} , which occurs with the increase of T_m . The optimal value of T_m is $19\text{ }^\circ\text{C}$ and the maximum COP_{tot} is 2.38, which is 4.4% higher than the minimum COP_{tot} . The absorption pressure of AB1 decreases with the increase of T_m . The concentration of the dilute solution at the outlet of AB1 decreases when the absorption temperature is constant, so it can be driven by a lower temperature at the same generation pressure. The concentration of dilute solution entering G2 remains unchanged but the generation pressure decreases, making both T_{G2} and T_{G1} increase. CS is the evaporator for the CO_2 transcritical subsystem. With the increase of T_m , the power consumption of COMP is gradually reduced, and the performance of the CO_2 transcritical subsystem is

then improved. Adjusting T_m is beneficial for reducing the input temperature of G1 and G2, which means more discharge heat can be recovered by a two-stage absorption refrigeration system. In a word, T_m has a significant impact on the performance of the CTTA system, and so it is necessary to match T_m reasonably.

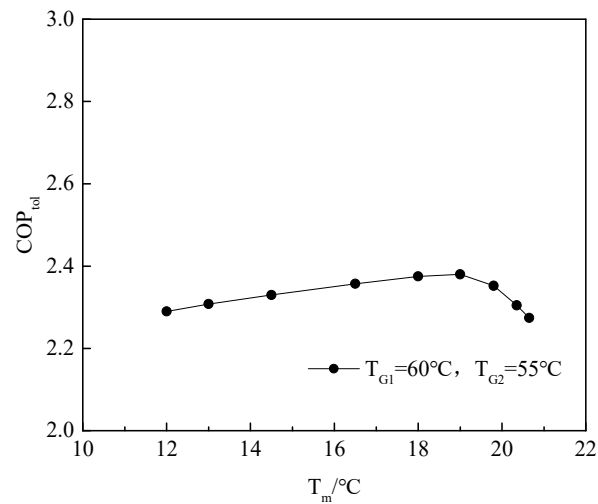


Figure 5. Effects of T_m on CTTA system performance.

Figure 6 shows the effects of T_{G2} on COP_{tot} and COP_{ch} , while the other parameters are the same as in the design conditions mentioned above. It can be seen that the CTTA system has an optimal value of T_{G2} in the obtaining of high COP. The maximum value of COP_{tot} and COP_{ch} is 3.70 and 2.90, respectively, when T_{G2} is 58 °C. The mass flow rate of water vapor generated at G2 increases with the increase of T_{G2} , so the refrigeration capacity increases, which leads to an increase in COP_{ch} and COP_{tot} . With the further increase of T_{G2} , the water vapor cannot be totally condensed at CS. Thus, the outlet quality in CS gradually increases after the mixture process, which leads to the increase of throttling loss at TV3. COP_{tot} and COP_{ch} then decline. Meanwhile, the traditional absorption refrigeration system cannot work normally when the generation temperature is below 58 °C. The refrigeration capacity is entirely generated by the input mechanical work, and so COP_{ch} increases. When T_{G2} is higher than 58 °C, the refrigerating capacity generated by the absorption system gradually increases, leading to the rapid decline of COP_{ch} . The maximum COP_{tot} is 27.6% higher than the maximum COP_{ch} , and 34.5% higher than COP_t , which shows the advantage of utilizing the exhaust heat of GC.

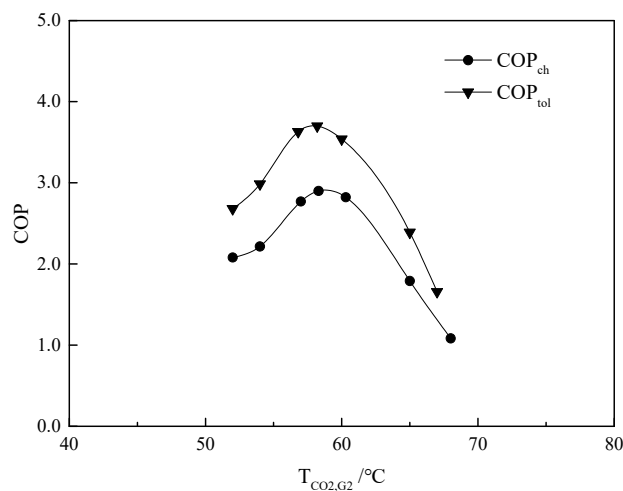


Figure 6. Effects of T_{G2} on CTTA system performance.

The effects of T_E on COP_{ch} and COP_{tol} are depicted in Figure 7, while the other parameters are the same as design conditions. COP_{ch} and COP_{tol} keep rising as T_E increases. The maximum COP_{tol} is 3.84 which is 21.5% higher than COP_{ch} , and 39.6% higher than COP_t . T_E causes the increase in the concentration difference of solutions in AB2, which leads to the increase of the mass flow rate of refrigerant in G2 and the refrigeration capacity in E. Therefore, the performance of the absorption refrigeration subsystem rises first, and COP_{tol} increases as well. However, when T_E is higher than 6 °C, more water vapor is generated; this vapor cannot be totally condensed in CS, so the quality of CS at the outlet gradually increases after the mixture process, which leads to the increase of throttling loss at TV3. Thus, the performance of the absorption refrigeration subsystem decreases and the slope of the COP_{tol} curve goes down.

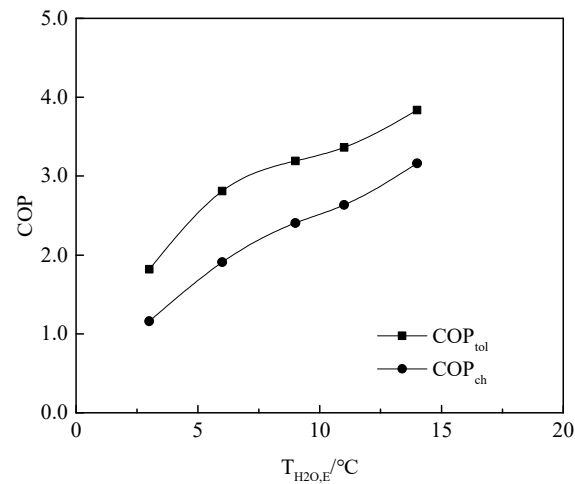


Figure 7. Effects of T_E on CTTA system performance.

The effects of T_C are shown in Figure 8, while the other parameters are the same as those of the design conditions. With the increase of T_C , the heat transfer efficiency in C decreases, which causes an increase in refrigerant quality at C outlet and CS. Then, the refrigeration capacity declines and the performance of the absorption subsystem decreases. Meanwhile, the conventional two-stage absorption refrigeration system cannot be driven when T_{C2} is lower than 60 °C. The increase of T_C will reduce the performance of the CO_2 transcritical subsystem, and the COP_{ch} shows a similar trend with COP_{tol} . The maximum COP_{tol} is 4.01 and COP_{ch} is 3.01 in the T_C of 28 °C. The maximum COP_{tol} is 33.2% higher than COP_{ch} , and 45.8% higher than COP_t .

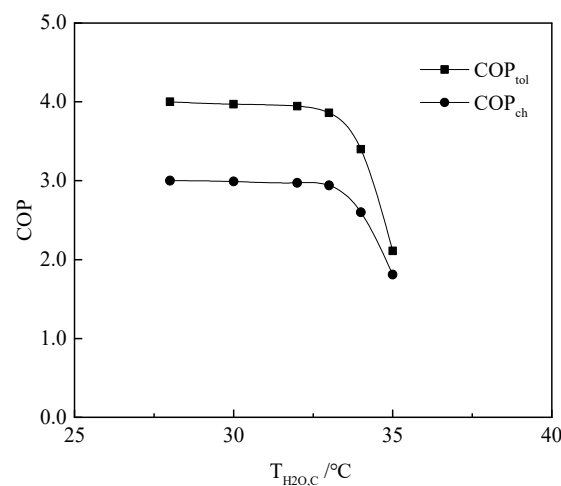


Figure 8. Effects of T_C on CTTA system performance.

The effects of T_{AB} on COP_{ch} and COP_{tol} are illustrated in Figure 9, and the other parameters are the same as the design conditions. The heat load on the refrigeration water side of the absorber decreases due to the increase of T_{AB} , which causes the vapor flow from G1 and G2 to decrease. Therefore, the refrigeration capacity of the CTTA system is reduced and COP decreases with the increase of T_{AB} . But because the vapor generated by G1 and G2 can be completely condensed in CS, the throttling loss of the system is reduced. In addition, the decrease of the vapor flow rate will also enhance the heat transfer efficiency of heat exchangers. Therefore, when T_{AB} is below 28 °C, the COP_{tol} is still high; when T_{AB} is greater than 28 °C, the system performance starts to decrease; and when T_{AB} is below 28 °C, the generation temperature is low, so the COP_a is 0 and the COP_{ch} decreases with the increase of T_{AB} . The maximum COP_{tol} of 3.78 and the maximum COP_{ch} of 3.02 are obtained at T_{AB} of 28 °C.

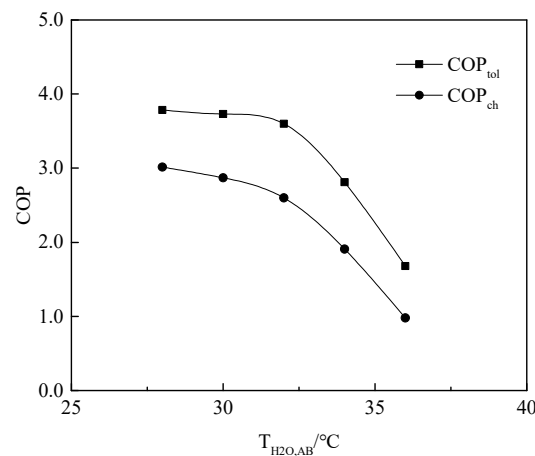


Figure 9. Effects of T_{AB} on CTTA system performance.

The effects of T_{air} on COP_{ch} and COP_{tol} are shown in Figure 10, while the other parameters are consistent with the design conditions. As T_{air} increases, an optimal value of T_{air} exists, that can be used to obtain the maximum COP. The temperature of CO_2 at the GC outlet increases as T_{air} rises, resulting in increases of T_{G1} and T_{G2} . So the performance of the absorption subsystem is increased first. In the CO_2 transcritical subsystem, the increase in T_{air} causes the temperature of CO_2 at the outlet of GC to increase, resulting in a decrease in CO_2 flow rate, refrigeration capacity, and COP of the CO_2 transcritical subsystem. There is therefore an optimal T_{air} to maximize the COP_{tol} . For COP_{ch} , an increase in T_{air} leads to a temperature increase in CS; an optimum value of T_m also exists, so the COP_{ch} increases first and then decreases. The optimal value of T_{air} is 58 °C, when the maximum COP_{ch} is 3.32 and the maximum COP_{tol} is 4.32, which is 30.1% higher than COP_{ch} .

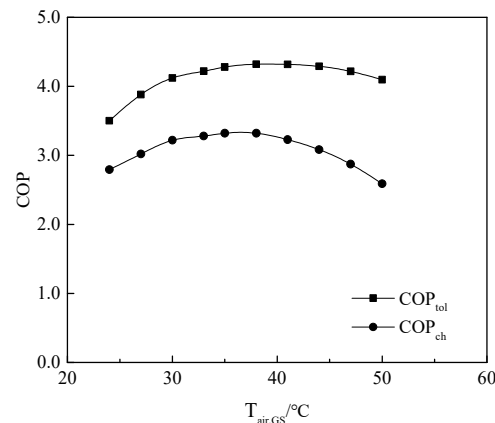


Figure 10. Effects of T_{air} on CTTA system performance.

The effects of P_c on COP_{ch} and COP_{tol} are displayed in Figure 11, while the other parameters are the same as the design conditions. There is also an optimal value for P_c to maximize system performance. Both the power consumption and the refrigeration capacity of the CO_2 transcritical subsystem increase as P_c increases. The increase in refrigeration capacity of the CO_2 transcritical subsystem allows the water vapor to be completely condensed in CS, resulting in an increase in the refrigeration capacity of the absorption subsystem. When P_c is lower than the optimal value, the refrigeration capacity contributed by the absorption subsystem is relatively high, so COP_{tol} gradually increases. And when P_c is higher than the optimal value, the refrigeration capacity generated by the CO_2 transcritical subsystem input mechanical work increasingly becomes larger, leading to a reduction in the performance of the CTTA system. The optimal value of P_c is 9.1 kPa when the maximum COP_{tol} is 4.18 and the corresponding COP_{ch} is 3.32.

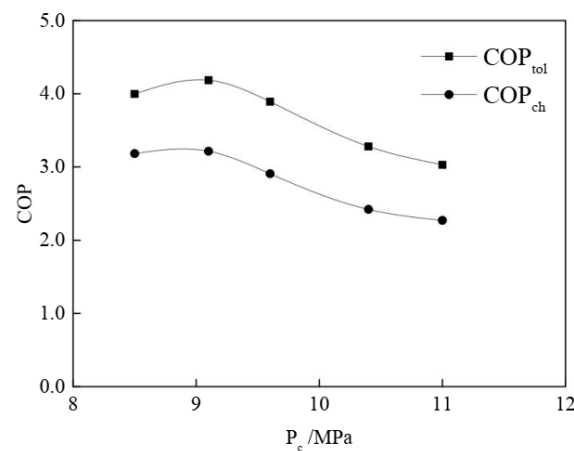


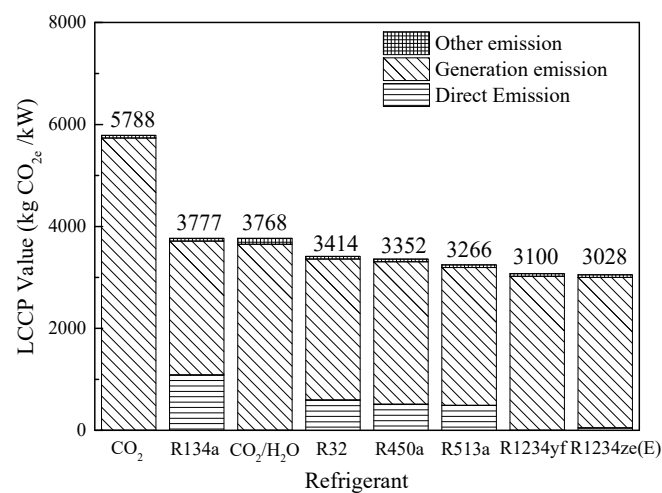
Figure 11. Effects of P_c on CTTA system performance.

The determination of the optimal parameters is essential to improve the performance of the CTTA system and reduce its carbon emissions. In the three optimal operating conditions of Figures 6, 10 and 11, COP_{tol} improved by 34.5–57.1% over COP_t . The coupling method to GC is the major difference between the CTTA system and the conventional hybrid refrigeration system. Optimizing T_{air} can improve 27.6% of the COP_{tol} , compared to COP_{ch} , while optimizing T_{G2} can improve 13.2%. The highest COP_{tol} of 4.32 indicates that the proposed coupling method provides a significant improvement when compared to conventional hybrid systems, and accordingly will result in a lower carbon emission of the refrigeration system, making the application of CO_2 to air conditioning in low carbon emission buildings more competitive.

To demonstrate the potential of the CTTA system to contribute to air conditioning in low carbon emission buildings, the LCCP method is used to compare the CTTA system with a BCT system and seven conventional refrigeration systems that use CO_2 , R134a, R32, R450a, R513a, R1234yf, and R1234ze(E), respectively. The coefficients required in the calculation of the LCCP values are obtained from the IIR guidelines [10], and the COP reference values for each system are obtained from the literature [40–44]. The main data required for the calculations are listed in Table 4. And the calculation results are shown in Table 4 and Figure 12.

Table 4. Reference values used for LCCP calculation and calculation results.

	CO ₂	R134a	R32	R450a	R513a	R1234yf	R1234ze(E)
COP	2.75 [40]	6.00 [41]	5.70 [42]	5.64 [43]	5.83 [44]	5.22 [43]	5.34 [43]
L (yr)	15	15	15	15	15	15	15
ALR (%)	5	5	5	5	5	5	5
EOL (%)	15	15	15	15	15	15	15
Adp. GWP (kg CO _{2e} /kg)	0	1.6	/	/	/	3.3	/
EM (kg CO _{2e} /kWh)				0.973			
RFM (kg CO _{2e} /kg)	0	5	7.2	10	10	13.7	14
Direct emission (kg CO _{2e} /kW)	2	1087	595	486	492	1	4
Indirect emission (kg CO _{2e} /kW)	5786	2689	2832	2866	2774	3099	3024

**Figure 12.** LCCP evaluation of a refrigeration system with different refrigerants.

As seen in Figure 12, systems with low GWP refrigerants all show a considerable reduction in direct carbon emissions, when compared to R134a systems. Direct carbon emission of the BCT system, for example, is comparable to the R1234yf and R1234ze(E) systems, and is seen to be significantly reduced when compared to the R134a and R32 systems. It shows that CO₂ used for air conditioning has a huge advantage in direct carbon emissions, compared to other low GWP refrigerants. Indirect carbon emissions account for the largest share of the LCCP value, of which carbon emissions generated from power generation are the main cause.

The BCT system has the highest LCCP value of 5788 kg CO_{2e}/kW, as its COP is much lower than the other systems. It also shows that the BCT system for air conditioning is still confronted by challenges. The R134a system already has a high COP at present, so its indirect emissions are 40% lower than the BCT system. But the higher GWP of the refrigerant also makes its LCCP value higher than the other systems. With a higher COP, the CTTA system has an LCCP value of 3768 kg CO_{2e}/kW, which is not only 53.6% lower than the BCT system, but also lower than the R134a system, which shows the potential of the CTTA system for air conditioning. R450a and R513a still have higher GWP, and their direct carbon emissions are 400% higher than that of the CTTA system. The R1234yf and R1234ze(E) systems, which also have extremely low GWP, have the lowest LCCP values, 18% and 20% lower than the CTTA system, respectively, which is because their COP is also higher. The LCCP values of the R32, R450a and R513a systems are reduced compared to the R134a system, but are slightly higher than the R1234yf and R1234ze(E) systems. From the perspective of the LCCP value, the CTTA system achieves ultra-low carbon emissions (compared to conventional BCT systems), greatly improves competitiveness when using CO₂ for air conditioning, and also has the advantages of natural refrigerants. In order to

underscore the potential for CTTA system applications, comparisons should be made with the same models and operational conditions. Unfortunately, few studies of the life cycle analysis for related systems can be found. The lack of comparative data obtained in the same operational conditions clearly challenges efforts to accurately evaluate CTTA systems. However, there is a growing interest in a trend that seeks to demonstrate application potential by undertaking life cycle analysis.

It is worth mentioning that the CTTA system has huge potential to reduce carbon emissions, as the efficiency of the CO₂ transcritical subsystem could be further improved. In the Introduction, performance enhancement methods for CO₂ transcritical refrigeration systems were discussed [14–17]. The COP of a BCT subsystem could be enhanced by the above methods. The potential of the CTTA system to reduce the LCCP value could also be estimated by calculating the improvement in COP by using the above methods. The COP of the CTTA system is evaluated in Table 5. The LCCP values are also compared with other conventional systems in Figure 13, and are summarized in Table 5.

Table 5. Potential of the CTTA system to reduce of LCCP values.

New CTTA System		COP Improvement (%)	LCCP Value (kg CO _{2e} /kW)	Improvement, Compared to Traditional Refrigerant Systems (%)			
Potential Case				R134a	R32	R1234yf	R1234ze(E)
1	Discharge pressure optimization [15]	8.8	3473	8.0	−1.7	−12.0	−14.7
2	Refrigerant discharge optimization [14]	10.1	3433	9.1	−0.5	−10.8	−13.4
3	Ejector expansion cycle [16]	20.0	3160	16.3	7.4	−1.9	−4.4
4	Ejector-cascade cycle [17]	30.0	2926	22.5	14.3	5.6	−3.4

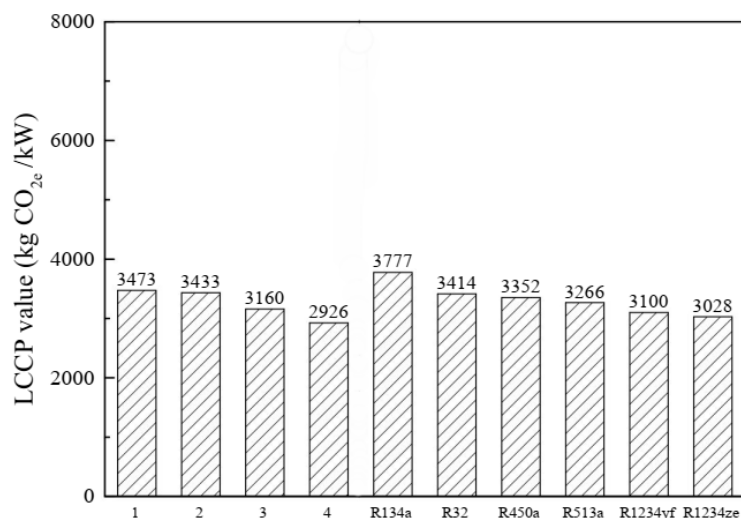


Figure 13. LCCP potentials of the CTTA system, compared with conventional systems.

For example, it is only after the key parameters of the CO₂ transcritical cycle are optimized that the potential carbon emissions of the CTTA system could be reduced to 3433 kg CO_{2e}/kW, which is 9.1% lower than the R134a system and equivalent to the R32 system [14]. When the CO₂ subsystem uses ejector to lift COP, the carbon emissions of the CTTA system might be reduced to 3160 kg CO_{2e}/kW [16], which is comparable to the carbon emissions of the R1234yf system. Further, with the use of the ejector-cascade cycle [17], the potential carbon emissions of the CTTA system are reduced to 2926 kg CO_{2e}/kW. This carbon emission is 3.4% lower than the R1234ze(E) system, demonstrating the prospect that the CTTA system could positively contribute to air conditioning applications in ultra-low carbon emission buildings.

5. Conclusions

As a natural refrigerant with extremely low GWP, and which is environmentally friendly, easily available and low cost, CO₂'s potential application to refrigeration systems is very promising. Conventional CO₂ transcritical refrigeration systems have relatively low COP, which means they generate massive indirect carbon emissions. In this study, a novel CO₂ transcritical/two-stage absorption hybrid refrigeration system is investigated on the basis of the COP and LCCP values. After the effects of key parameters on the COP_{tol} of the CTTA system are analyzed, the optimal parameters are determined by observing the Figures of COP-P and COP-T. The LCCP value of the CTTA system is compared with seven conventional refrigeration systems, by using CO₂, R134a, R32, R450a, R513a, R1234yf, and R1234ze(E) as refrigerants, respectively. The potential of the CTTA system to reduce the LCCP value is also estimated by referring to four potential cases. The conclusions of the study are as follows:

1. Optimal values of T_m , T_{G2} , T_{air} , and P_c exist for obtaining the maximum COP_{tol}.
2. The CTTA system has a notable improvement of 57.1% in COP_{tol}, when compared to the BCT system.
3. The CTTA system has an equivalent carbon emission to the R134a system, which is 53.6% lower than the BCT system.
4. Ultra-low carbon emissions could be obtained for the CTTA system, which could be reduced to 2926 kg CO_{2e}/kW, a total 3.4% lower than the R1234ze(E) systems.

The above findings indicate that the CTTA system leads to an obvious improvement in the low COP of BCT systems for air conditioning, and also achieves ultra-low carbon emissions. It can therefore be considered alongside R1234yf and R1234ze refrigeration systems, and should be seen as providing a potential alternative for the transformation and upgrading of air conditioning systems in the future.

Author Contributions: Y.H.: Conceptualization, investigation, methodology, writing—original draft; Y.Z.: data curation, resources; J.Z.: formal analysis, visualization; Q.C.: validation; L.Z.: writing—review & editing. All authors have read and agreed to the published version of the manuscript.

Funding: This work was supported by the Key Research and Development Program in Zhejiang Province (No. 2023C01251).

Data Availability Statement: Data are contained within the article.

Conflicts of Interest: Authors Yufu Zheng and Jianguang Zhao were employed by the company Zhejiang Shike Auto Parts Co., Ltd. The remaining authors declare that the research was conducted in the absence of any commercial or financial relationships that could be construed as a potential conflict of interest.

Nomenclature

	Nomenclature	Unit		Subscripts
Adp.GWP	GWP of atmospheric degradation product	kg CO _{2e} /kg	1,2,3	State point
AEC	Annual energy consumption	kWh	a	Absorption system
Cr	Refrigerant charge	kg	ch	Conventional hybrid system
EM	Power plant emission factor	kg CO _{2e} /kWh	exp	Experimental result
EOL	End-of-life refrigeration leakage	%	m	Intermedia
GWP	Global Warming Potential	kg CO _{2e} /kg	sim	Simulation result
h	Enthalpy	kJ/kg	tol	Total
L	Average lifetime of equipment	year		Abbreviations
M	Mass of unit	kg	AB	Absorber
MM	CO _{2e} produced/material	kg CO _{2e} /kg	BCT	Basic CO ₂ transcritical
<i>m</i>	Mass flow rate	kg/s	C	Condenser
mr	Mass of recycle material	kg	COMP	Compressor

Q	Rated heat load	kW	CS	Condensing subcooler
Q _e	Refrigeration capacity	kW	CTTA	CO ₂ transcritical/two-stage absorption
RM	CO _{2e} produced/Recycled Material	kg CO _{2e} /kg	E	Evaporator
RFM	Refrigerant manufacturing emissions	kg CO _{2e} /kg	G	Generator
RFD	Refrigerant disposal emissions	kg CO _{2e} /kg	GC	Gas cooler
T	Temperature	°C	GWP	Global warming potential
W	Input power	kW	IHX	Internal heat exchanger
			LCCP	Life cycle climate performance
			SHX	Solution heat exchanger
			SP	Solution pump
			TV	Throttling valve
			DMS	Dedicated mechanical subrefrigeration

References

- Li, J. Towards a low-carbon future in China's building sector-A review of energy and climate models forecast. *Energy Policy* **2008**, *36*, 1736–1747. [[CrossRef](#)]
- Makhnatch, P.; Mota-Babiloni, A.; López-Belchí, A.; Khodabandeh, R. R450A and R513A as lower GWP mixtures for high ambient temperature countries: Experimental comparison with R134a. *Energy* **2019**, *166*, 223–235. [[CrossRef](#)]
- Li, Y.X.; Zhang, Z.Y.; De An, M.; Gao, D.; Yi, L.Y.; Hu, J.X. The estimated schedule and mitigation potential for hydrofluorocarbons phase-down in China. *Adv. Clim. Chang. Res.* **2019**, *10*, 174–180. [[CrossRef](#)]
- Lemmon, E.W.; Huber, M.L.; McLinden, M.O.; Bai, W. *REFPROP, NIST Standard Reference Database 23; Version 9.1*; National Institute of Standards and Technology: Gaithersburg, MD, USA, 2013.
- Bhamidipati, A.; Pendyala, S.; Prattipati, R. Performance evaluation of multi pressure refrigeration system using R32. *Mater. Today Proc.* **2020**, *28*, 2405–2410. [[CrossRef](#)]
- Tanaka, K.; Higashi, Y. Thermodynamic properties of HFO-1234yf (2,3,3,3-tetrafluoropropene). *Int. J. Refrig.* **2010**, *33*, 474–479. [[CrossRef](#)]
- Navarro-Esbri, J.; Molés, F.; Barragán-Cervera, Á. Experimental analysis of the internal heat exchanger influence on a vapour compression system performance working with R1234yf as a drop-in replacement for R134a. *Appl. Therm. Eng.* **2013**, *59*, 153–161. [[CrossRef](#)]
- Gaurav; Kumar, R. Computational energy and exergy analysis of R134a, R1234yf, R1234ze and their mixtures in vapour compression system. *Ain Shams Eng. J.* **2018**, *9*, 3229–3237. [[CrossRef](#)]
- Makhnatch, P.; Mota-Babiloni, A.; Khodabandeh, R. Experimental study of R450A drop-in performance in an R134a small capacity refrigeration unit. *Int. J. Refrig.* **2017**, *84*, 26–35. [[CrossRef](#)]
- International Institute of Refrigeration (IIR). *Guideline for Life Cycle Climate Performance January 2016*; International Institute of Refrigeration: Paris, France, 2016; pp. 1–26.
- Choi, S.; Oh, J.; Hwang, Y.; Lee, H. Life cycle climate performance evaluation (LCCP) on cooling and heating systems in South Korea. *Appl. Therm. Eng.* **2017**, *120*, 88–98. [[CrossRef](#)]
- Lee, H.; Troch, S.; Hwang, Y.; Radermacher, R. LCCP evaluation on various vapor compression cycle options and low GWP refrigerants. *Int. J. Refrig.* **2016**, *70*, 128–137. [[CrossRef](#)]
- Yu, B.; Yang, J.; Wang, D.; Shi, J.; Chen, J. An updated review of recent advances on modified technologies in transcritical CO₂ refrigeration cycle. *Energy* **2019**, *189*, 116147. [[CrossRef](#)]
- Wang, A.; Yin, X.; Fang, J.; Cao, F. Refrigerant Distributions and Dynamic Migration Characteristics of the Transcritical CO₂ Air Conditioning System. *Int. J. Refrig.* **2021**, *130*, 233–241. [[CrossRef](#)]
- Song, Y.; Ye, Z.; Wang, Y.; Cao, F. The experimental verification on the optimal discharge pressure in a subcooler-based transcritical CO₂ system for space heating. *Energy Build.* **2018**, *158*, 1442–1449. [[CrossRef](#)]
- Lawrence, N.; Elbel, S. Comparison of CO₂ and R134a two-phase ejector performance for use in automotive air conditioning applications. *SAE Tech. Pap.* **2014**, *1*. [[CrossRef](#)]
- Tashtoush, B.; Megdoui, K.; Elakhdar, M.; Nehdi, E.; Kairouani, L. A comprehensive energy and exergoeconomic analysis of a novel transcritical refrigeration cycle. *Processes* **2020**, *8*, 758. [[CrossRef](#)]
- Megdoui, K.; Tashtoush, B.M.; Nahdi, E.; Elakhdar, M.; Kairouani, L.; Mhimid, A. Thermodynamic analysis of a novel ejector-cascade refrigeration cycles for freezing process applications and air-conditioning. *Int. J. Refrig.* **2016**, *70*, 108–118. [[CrossRef](#)]
- Liu, X.; Hu, Y.; Wang, Q.; Yao, L.; Li, M. Energetic, environmental and economic comparative analyses of modified transcritical CO₂ heat pump system to replace R134a system for home heating. *Energy* **2021**, *229*, 120544. [[CrossRef](#)]
- Chan, W.M.; Leong, Y.T.; Foo, J.J.; Chew, I.M.L. Synthesis of energy efficient chilled and cooling water network by integrating waste heat recovery refrigeration system. *Energy* **2017**, *141*, 1555–1568. [[CrossRef](#)]
- Jain, V.; Sachdeva, G.; Kachhwaha, S.S. Comparative performance study and advanced exergy analysis of novel vapor compression-absorption integrated refrigeration system. *Energy Convers. Manag.* **2018**, *172*, 81–97. [[CrossRef](#)]

22. Gibelhaus, A.; Fidorra, N.; Lanzerath, F.; Bau, U.; Köhler, J.; Bardow, A. Hybrid refrigeration by CO₂ vapour compression cycle and water-based adsorption chiller: An efficient combination of natural working fluids. *Int. J. Refrig.* **2019**, *103*, 204–214. [[CrossRef](#)]
23. He, Y.J.; Jiang, Y.Y.; Gao, N.; Chen, G.M.; Tang, L.M. Theoretical analyses of a new two-stage absorption-transcritical hybrid refrigeration system. *Int. J. Refrig.* **2015**, *56*, 105–113. [[CrossRef](#)]
24. Klein, S.A. *Engineering Equation Solver (EES) 1992–2014*; F-Chart Software: Middleton, WI, USA, 2020.
25. Herold, K.E. 99/01562 An analysis of the major variables impacting performance of absorption chillers and heat pumps. *Fuel Energy Abstr.* **1997**, *40*, 157. [[CrossRef](#)]
26. Chen, X.; He, Y.; Wang, Y.; Chen, G. Analysis of a hybrid system of liquid desiccant and CO₂ transcritical cycles. *Int. J. Refrig.* **2019**, *105*, 101–108. [[CrossRef](#)]
27. Mcneely, L.A. Thermodynamic properties of aqueous solutions of lithium-bromide. *ASHRAE Trans.* **1979**, *20*, 54–55.
28. Berlitz, T.; Plank, H.; Ziegler, F.; Kahn, R. An ammonia-water absorption refrigerator with a large temperature lift for combined heating and cooling. *Int. J. Refrig.* **1998**, *21*, 219–229. [[CrossRef](#)]
29. Span, R.; Wagner, W. A new equation of state for carbon dioxide covering the fluid region from the triple-point temperature to 1100K at Pressures up to 800 MPa. *J. Phys. Chem. Ref. Data.* **1996**, *6*, 1509–1596. [[CrossRef](#)]
30. Dai, Y. *The Technology and Application of Lithium Bromide Absorption Refrigeration*; Machinery Industry Press: Beijing, China, 1996. (In Chinese)
31. Pitla, S.S.; Groll, E.A.; Ramadhani, S. New correlation to predict the heat transfer coefficient in-tube cooling of supercritical CO₂ in horizontal macro-tubes. *Exp. Therm. Fluid Sci.* **2002**, *25*, 887–895. [[CrossRef](#)]
32. Huang, D.; Liang, Z.; Ding, G.; Zhang, C. Modeling and Performance Analysis of LFSN. *J. Chem. Ind. Eng.* **2002**, *53*, 832–836. [[CrossRef](#)]
33. Agrawal, N.; Bhattacharyya, S. Non-adiabatic capillary tube flow of carbon dioxide in a transcritical heat pump cycle. *Energy Convers. Manag.* **2007**, *48*, 2491–2501. [[CrossRef](#)]
34. Lockhart, R.; Martinelli, R. Proposed correlation of data for isothermal two-phase, two-component flow in pipes. *Chem. Eng. Prog. Symp. Ser.* **1949**, *45*, 39–48.
35. Yunho, H.; Reinhard, R. Performance Measurement of CO₂ Heat Exchangers. *ASHRAE Trans.* **2005**, *111*, 306–316.
36. Boewe, D.; Bullard, C.; Yin, J.; Hrnjak, P. Contribution of internal heat exchanger to transcritical R744 cycle performance. *ASHRAE Trans.* **2001**, *2*, 189–198.
37. Mohammadi, S.M.H. Theoretical investigation on performance improvement of a low-temperature transcritical carbon dioxide compression refrigeration system by means of an absorption chiller after-cooler. *Appl. Therm. Eng.* **2018**, *138*, 264–279. [[CrossRef](#)]
38. Farsi, A.; Mohammadi, S.M.H.; Ameri, M. An efficient combination of transcritical CO₂ refrigeration and multi-effect desalination: Energy and economic analysis. *Energy Convers. Manag.* **2016**, *127*, 561–575. [[CrossRef](#)]
39. Yuan, Y.; Xianlong, W.; Yongjun, T. Performance investigation on double-lift LiBr absorption refrigerator in variable conditions. *Cryogenics* **2013**, *193*, 21–26.
40. Zhang, F.Z.; Jiang, P.X.; Lin, Y.S.; Zhang, Y.W. Efficiencies of subcritical and transcritical CO₂ inverse cycles with and without an internal heat exchanger. *Appl. Therm. Eng.* **2011**, *31*, 432–438. [[CrossRef](#)]
41. Janković, Z.; Atienza, J.S.; Suárez, J.A.M. Thermodynamic and heat transfer analyses for R1234yf and R1234ze(E) as drop-in replacements for R134a in a small power refrigerating system. *Appl. Therm. Eng.* **2015**, *80*, 42–54. [[CrossRef](#)]
42. Bolaji, B.O. Experimental study of R152a and R32 to replace R134a in a domestic refrigerator. *Energy* **2010**, *35*, 3793–3798. [[CrossRef](#)]
43. Mendoza-Miranda, J.M.; Mota-Babiloni, A.; Ramírez-Minguela, J.J.; Muñoz-Carpio, V.D.; Carrera-Rodríguez, M.; Navarro-Esbrí, J.; Salazar-Hernández, C. Comparative evaluation of R1234yf, R1234ze(E) and R450A as alternatives to R134a in a variable speed reciprocating compressor. *Energy* **2016**, *114*, 753–766. [[CrossRef](#)]
44. Llopis, R.; Sánchez, D.; Cabello, R.; Catalán-Gil, J.; Nebot-Andrés, L. Experimental analysis of R-450A and R-513A as replacements of R-134a and R-507A in a medium temperature commercial refrigeration system. *Int. J. Refrig.* **2017**, *84*, 52–66. [[CrossRef](#)]

Disclaimer/Publisher's Note: The statements, opinions and data contained in all publications are solely those of the individual author(s) and contributor(s) and not of MDPI and/or the editor(s). MDPI and/or the editor(s) disclaim responsibility for any injury to people or property resulting from any ideas, methods, instructions or products referred to in the content.